Journal of Chemistry and Technologies, 2025, *33*(1), 262-270

Journal of Chemistry and Technologies

pISSN 2663-2934 (Print), ISSN 2663-2942 (Online).

journal homepage: http://chemistry.dnu.dp.ua
editorial e-mail: chem.dnu@gmail.com

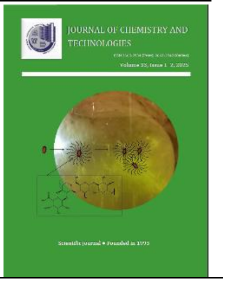

UDC 544.47

VIBRATIONAL RESONANCE DURING CO-OXIDATION ON PLATINUM CATALYST SURFACES

S. Siva Sakthi Pitchammal[1], Sheik Mohamed Abdul Kader[1], M. Mohamed Roshan[1],
Isravel Antony Danish[2], Veerapadran Chinnathambi[1*]

[1]*Department of Physics, Sadakathullah Appa College, Tirunelveli-627 011, Tamilnadu, India*
[2]*Department of Chemistry, Sadakathullah Appa College, Tirunelveli-627 011, Tamilnadu, India*

Received 10 May 2024; accepted 12 December 2024; available online 15 April 2025

Abstract

Vibrational resonance is a nonlinear phenomenon in which two external signals, a low-frequency signal (ω) and a high-frequency signal (Ω), interact cooperatively, with Ω significantly larger than ω. This interaction strengthens the response of the weaker, low-frequency signal. In this paper, we investigate the application of vibrational resonance in a surface catalytic reaction model, specifically focusing on the oxidation of Carbon Monoxide (CO) on a platinum catalyst. By performing numerical simulations, we examine how the introduction of a low-frequency periodic signal superimposed on a high-frequency signal affects the catalytic reaction dynamics. The results reveal that vibrational resonance reduces the energy barrier for CO oxidation, which leads to enhanced reaction rates compared to conditions without resonance. This effect occurs due to the optimal synchronization of the two frequencies, which facilitates more efficient energy transfer and reaction processes. Ultimately, this research demonstrates that vibrational resonance can significantly improve catalytic activity in CO oxidation reactions, offering insights into optimizing catalytic performance.

Keywords: CO-oxidation; platinum catalyst; vibrational resonance; chaotic oscillation; response amplitude; perturbation.

КОЛИВАЛЬНИЙ РЕЗОНАНС ПІД ЧАС ОКИСНЕННЯ СО НА ПОВЕРХНІ ПЛАТИНОВОГО КАТАЛІЗАТОРА

С. Сіва Сакті Пітчамал[1], Шейх Мохамед Абдул Кадер[1], М. Мохамед Рошан[1],
Ісравел Ентоні Даніш[2], Веерападран Чіннатхамбі[1]

[1]*Кафедра фізики, Коледж Садакатхулла Аппа, Тірунельвелі-627 011, Тамілнаду, Індія*
[2]*Кафедра хімії, Коледж Садакатхулла Аппа, Тірунельвелі-627 011, Тамілнаду, Індія*

Анотація

Вібраційний резонанс – нелінійне явище, що проявляється як кооперативний ефект між двома зовнішніми сигналами: низькочастотним (ω) і високочастотним (Ω), де Ω >> ω. Це явище підсилює слабший сигнал. У цій статті досліджено коливальний резонанс у моделі поверхневої каталітичної реакції з особливим акцентом на окисненні монооксиду вуглецю (СО). За допомогою чисельного моделювання ми спостерігаємо поведінку коливального резонансу в моделі каталітичної реакції, коли низькочастотний періодичний сигнал накладається на високочастотний сигнал, керуючи таким чином системою. Цей посилений коливальний резонанс ефективно знижує енергетичний бар'єр для реакцій окиснення СО, що призводить до збільшення швидкості реакції порівняно з нерезонансними умовами. По суті, резонансна динаміка створює оптимальні умови для окиснення СО на поверхні платинового каталізатора, що приводить до покращення каталітичної активності.

Ключові слова: окиснення СО; платиновий каталізатор; вібраційний резонанс; хаотичні коливання; амплітуда відгуку; збурення.

**Corresponding author: e-mail: veerchinnathambi@gmail.com*

doi: 10.15421/jchemtech.v33i1.303777

Introduction

Over the past decade, there has been significant interest in studying the complex dynamics and chemistry of oscillating reactions under external perturbations. This exploration has yielded various outcomes, including period-doubling bifurcation leading to chaotic motion, quasi-periodic routes to chaos, coexistence of multiple attractors, hysteresis, stochastic resonance, and vibrational resonance [1–3]. Among these, CO-oxidation on platinum (Pt) catalyst surfaces has emerged as an intriguing interdisciplinary field within natural sciences. Since Langmuir's seminal investigations [4], the oxidation of CO over platinum has stood out as a classic example of a heterogeneous catalytic reaction. Its apparent simplicity in mechanism, coupled with the richness of spatiotemporal behavior and practical significance, renders it a generic model system [5–8]. Resonance, as observed in reactions on catalytic surfaces under period forcing of operating variables, is an intriguing phenomenon. The imposition of external forces on nonlinear systems can dramatically alter their time-averagedbehavior. When a nonlinear system experiences simultaneous multiple excitations, its response to slowly varying excitation closely correlates with the fast-varying excitation. This phenomenon is termed *Vibrational Resonance* (VR), which shares similarities with *Stochastic Resonance (SR)* but involves the high-frequency input force instead of noise [9,10]. Stochastic resonance phenomena have been extensively explored in chemical reaction models. For instance, Yang et al. [11,12] investigated stochastic resonance in the catalytic reduction of NO with CO on $Pt(100)$ surfaces and the surface catalytic oxidation of carbon monoxide. Gong et al. explored internal noise stochastic resonance in CO oxidation on nanometer-sized palladium particles [9]. Ma et al. [13] analyzed two-parameter coherent resonance behaviorin the catalytic oxidation of CO on platinum surfaces.

In this paper, we analyze the occurrence of vibrational resonance (VR) in the CO-oxidation reaction over a platinum catalytic surface model. The VR phenomenon comprises three basic elements: (i) nonlinear systems, (ii) slowly varying excitation (characteristic signal), and (iii) fast varying excitation (auxiliary signal). Through the interaction of these elements, VR emerges via a weak, low-frequency, or slowly varying signal. Therefore, the development of vibrational theory is crucial for detecting and amplifying weak signals. VR in CO-oxidation over Pt catalyst surfaces refers to a phenomenon in which the vibrational modes of carbon monoxide (CO) molecules adsorbed on a platinum (Pt) catalyst surface are excited and enhanced, leading to more efficient catalytic oxidation of CO to carbon dioxide(CO_2). The phenomenon of v*ibrational resonance* (VR) was first reported by Landa and McClintock [14]. Subsequently, Gitterman [15] analyzed a bistable system and provided an analytical explanation for the occurrence of VR. Later, Blekhman and Landa [16] conducted a more specific analytical study on VR in overdamped and underdamped Duffing oscillators. The occurrence of VR has been analyzed in a diverse range of model systems, both theoretically, numerically, and experimentally, spanning various fields such as neuroscience [17–19], plasma physics [20–22], laser physics [23–25], acoustics [26–28], and chemical kinetics [29–31].

The paper is structured as follows: Section 2 furnishes information about the model, elucidating the various steps entailed in the kinetic scheme. This section also presents the mathematical formulation of the kinetic scheme. In Section 3, we conduct a numerical analysis of the vibrational resonance phenomenon resulting from the application of biperiodic forces on the kinetic scheme. For a specific set of parameter values in the model, we demonstrate the occurrence of period-doubling cascades, attractor coexistence, and chaos. Finally, Section 4 comprises the conclusions drawn from the present study.

Kinetic model

The oxidation of carbon monoxide on platinum (*Pt)* catalyst surfaces stands as one of the most frequently employed model systems for investigating nonlinear effects in hetero-geneous catalysis. Previous studies have reported multiple steady states and various types of nonlinear dynamic regimes, including periodic, quasiperiodic, and chaotic oscillations in CO oxidation [32–38]. In recent years, increased attention has been directed towards studying resonant behaviors in catalytic CO-oxidation processes. Within a catalytic process, the reaction unfolds through a sequence of elementary steps, encompassing adsorption, surface diffusion, and chemical rearrangement (involving bond breaking, bond formation, and molecular rearrangement) of adsorbed intermediates, followed by product desorption.

The catalytic oxidation of CO on platinum typically adheres to the Langmuir-Hinshelwood mechanism [39,40], wherein both CO and oxygen must first adsorb onto the catalyst surfacebefore the conversion to CO_2 can occur. The stages involving reversible CO adsorption, O_2 adsorption, CO oxidation, and CO_2 desorption are considered as follows:

$$\text{Pt (s) + CO (g)} \underset{k_{-1}}{\overset{k_1}{\rightleftarrows}} \text{Pt - CO (s)} \tag{1}$$

$$\text{Pt (s) + } \tfrac{1}{2}O_2\text{(g)} \underset{K_{-2}}{\overset{K_2}{\rightleftarrows}} \text{2Pt - O (s)} \tag{2}$$

$$\text{Pt – CO (s) + Pt - O (s)} \overset{K_3}{\rightarrow} \text{Pt (s) + Pt – O - CO(s)} \tag{3}$$

$$\text{Pt – O – CO (s)} \underset{k_{-4}}{\overset{k_4}{\rightleftarrows}} \text{Pt (s) + CO}_2\text{ (g)} \tag{4}$$

The above catalytic reactions may be described by the following dimensionless form,

$$\dot{x}=2k_1z_2-2k\text{-}1\ x_2-k_3\ xy,$$
$$\dot{y}=k_2z-k\text{-}2\ y-k_3\ xy, \tag{5}$$
$$\dot{s}=k4\ (z-\lambda s).$$

Where z=1−x−y−s and $\lambda = k_{-4}/k_4$. The underlying reaction scheme is studied in ref. [39; 40]. In Eq.(5), x and y represent the dimensionless concentration of CO and O absorbed in the surface, respectively, and z denotes the dimensionless concentration of the subsurface oxygen. k_1, k_2, k_3 and k_4 are the rate constants. With two external periodic perturbation, Eq. (5) can be written as

$$\dot{x}=2k1z2-2k\text{-}1\ x2-k3\ xy + f \sin \omega t + g \sin\Omega t,$$
$$\dot{y}=k2\ z-k\text{-}2\ y-k3\ xy, \tag{6}$$
$$\dot{s}=k4\ (z-\lambda s).$$

Where Ω >> ω. In Eq. (6), $f \sin \omega t$ is the lower frequency signal component with the amplitude (f) and frequency (ω) and $g \sin \Omega t$ is the high-frequency component with the amplitude g and frequency Ω. In the following sections we analyze the occurrence of VR phenomenon in Eq. (6) by numerical simulation.

Vibrational resonance

The concept of vibrational resonance (VR) in catalysis has been the subject of extensive study in recent years. It offers valuable insights into the fundamental mechanisms underlying catalytic reactions and presents opportunities for optimizing catalyst performance. Understanding and controlling vibrational resonance processes have the potential to lead to the development of more efficient and selective catalysis for various industrial applications, including automotive catalytic converters and environmental remediation. In our numericalstudy, we select the amplitude (g) of the high-frequency signal as the control parameter, and the response behavior is characterized by one of the state parameters, denoted as x.

$$Q = \sqrt{Q_s^2 + Q_c^2}\ /\ \text{f},$$
$$\text{where } Q_s = \frac{2}{nT}\int_0^{nT} x(t) \sin \omega t$$
$$Q_c = \frac{2}{nT}\int_0^{nT} x(t) \cos \omega t \tag{7}$$

where $T = 2\pi/\omega$ and n is taken as 500.

To numerically analyze Eq. (6), we employ the fourth-order Runge-Kutta scheme with a time step size of $\Delta t = 0.01T$, where $T = 2\pi/\omega$. The simulation is conducted over a time interval $T_s = nT$, where n (with values such as 1, 2, 3, etc.) denotes the number of complete oscillations. From the numerical solution x(t) of Eq. (6), the response amplitude Q is computed from the Eq. (7). In our numerical analysis, we fix the rate constants of the reaction model (Eq. 6) as follows: $k_1 = 2.5$, $k_{-1} = 1.0$, $k_3 = 10.0$, $k_{-2} = 0.1$, $k_2 = 1.5$, $k_4 = 2.5$, $k_{-4} = 1.0$ and $\lambda = 0.4$. In the numerical calculations, the initial state variables are fixed as $x = 0.1, y = 0.8$ and $s = 0.2$

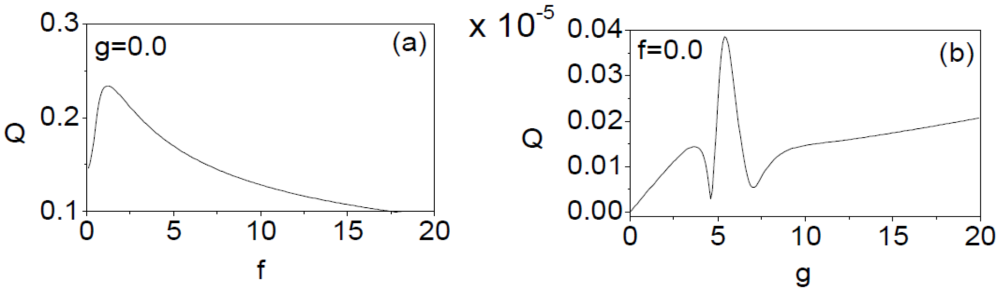

Fig. 1. (a) Variation in the numerically computed Q against the control parameter f with $\Omega = 20\omega$, $\omega = 1.0$, and $g = 0$. (b) Variation in the numerically computed Q against the control parameter $g$with $\Omega = 20\omega$, $\omega = 1.0$, and $f = 0$. The values of the rate constants of the reaction model (Eq. 6) are fixed as follows: $k_1 = 2.5$, $k_{-1} = 1.0$, $k_3 = 10.0$, $k_{-2} = 0.1$, $k_2 = 1.5$, $k_4 = 2.5$, $k_{-4} = 1.0$, and $\lambda = 0.4$. In the numerical calculations, the initial state variables are fixed as $x = 0.1, y = 0.8$, and $s = 0.2$

In the following, we compute the response amplitude Q with a low-frequency force only, a high-frequency force only, and with both forces combined. Figure 1 represents the variation in Q depending on f for $g=0.0$ and on g for $f=0.0$ when $\omega=1.0$. For $f=0$, Q is obtained as, $\sqrt{Q_S^2+Q_C^2}$ where Q_S and Q_C represent the Fourier coefficients of the output signal at the frequency Ω, and Q represents the amplitude of the response to the same frequency. Indeed, for $\Omega=20\omega$ with $\omega = 1.0$, the numerical results are shown in Fig. 1(a). From Fig. 1(a), we note that a single resonance peak is observed at $f=1.33$ with $Q_{max}=0.2322$, while for $f = 0.0$, we observe double resonance peaks at $g = 3.603$ with $Q_{max}= 0.0145\times10^{-5}$ and $g = 5.4887$ with $Q_{max}= 0.0378\ \times10^{-5}$, as clearly seen in Fig. 1(b). Subsequently, we analyze the effect of biperiodic force in the CO-oxidation on platinum surface (Eq .6) for the cases of $\Omega = \omega$ and $\Omega \neq \omega$. Firstly, we examine the effect of biperiodic force when $\Omega = \omega$, and the results obtained are shown in Fig. 2. Figure 2 shows the variation of response amplitude Q with g ranging from 0 to 30, with $\Omega = \omega = 1.0$, and the influence of the parameter f on the VR. From Fig. 2, we observe that the response amplitude Q gradually increases as g increases, and no resonances occur for all values of f. However, for the case of $\Omega >> \omega$, we observe VR, as presented in Fig. 3. The response amplitude Q increases with an increase in g, reaches a maximum, and then decreases with a further increase in g. The underlying phenomenon is VR, as the occurrence is due to the high-frequency component of the signal. Figure 3 illustrates the variation in Q with g for four different values of f (= 0.1, 0.5, 1.0, 2.0 respectively) with $\Omega = 20\omega$ and $\omega = 1.0$. From Fig. 3, we note that single resonance peaks are observed for all values of f, and the maximum of the response amplitude Q decreases as f increases. Additionally, the positions of peaks are shifted away from the origin. In the CO oxidation process, this type of resonance occurs when the frequency of CO adsorption and desorption matches the frequency of vibrational modes of the system. This resonance enhances the coupling between the adsorbate and the surface, leading to more efficient energy transfer and potentially accelerating the reaction rate.

When g varies from small values, vibrational resonance (VR) emerges for the case $\Omega >> \omega$. We observe that the persistence, form, maximum amplitude, and the value of g at resonance depend not only on f and ω but also on the rate constants k_1, k_2, and k_3 of the CO-oxidation over Pt surface scheme considered.

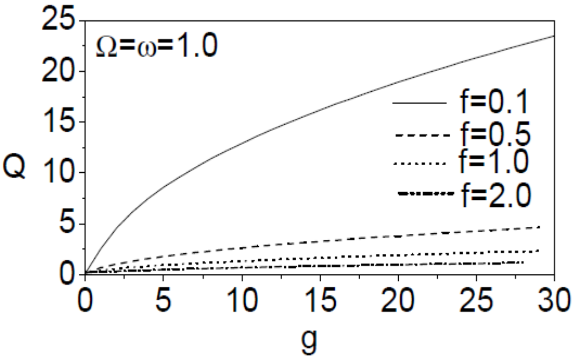

Fig. 2. Response amplitude Q versus g of the kinetic model (Eq. 6) for four values of f (=0.1, 0.5, 1.0, 2.0) respectively with $\Omega = \omega = 1.0$. The values of the rate constants and the initial conditions are fixed as given in Fig. 1.

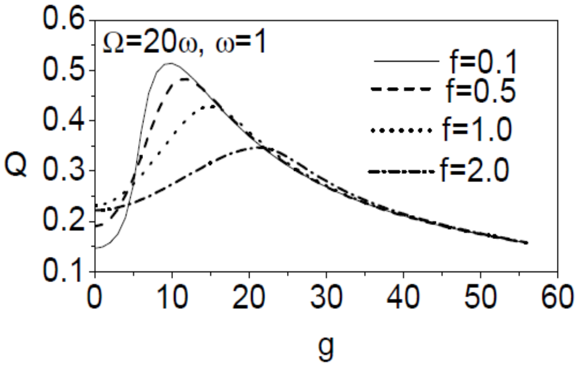

Fig. 3. Response amplitude Q versus g of the kinetic model (Eq. 6) for four values of f (=0.1, 0.5, 1.0, 2.0) respectively with $\Omega = 20\omega$ and $\omega = 1.0$. The values of the rate constants and the initial conditions are fixed as given in Fig. 1.

To illustrate the effect of the rate constant k_3, we plotted the response curve for four different values of k_3, as presented in Fig. 4. Figure 4 demonstrates the response curve when g varies from 0 to 150, with $\Omega = 20\omega$, $\omega = 2$, and $f = 0.1$, showcasing the influence of the parameter k_3 on *VR*.

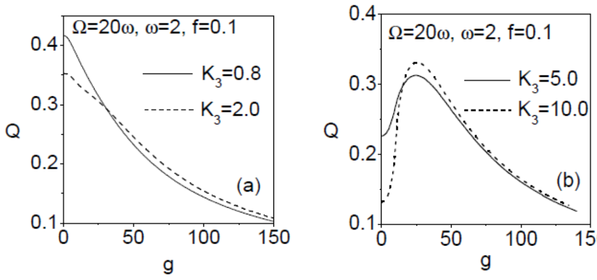

Fig. 4. Response amplitude Q versus g of the kinetic model (Eq. 6) for four values of k_3 (= 0.8, 2.0, 5.0, 10.0) respectively with $\Omega = 20\omega$, $\omega = 2.0$, and $f = 0.1$. The values of the rate constants of the reaction model (Eq. 6) are fixed as follows: $k_1 = 2.5$, $k_{-1} = 1.0$, $k_{-2} = 0.1$,$k_2 = 1.5$, $k_4 = 2.5$, $k_{-4} = 1.0$, and $\lambda = 0.4$. In the numerical calculations, the initial state variables are fixed as $x = 0.1$, $y = 0.8$, and $s = 0.2$

From Fig. 4(a), we observe that the maximum value of the response amplitude decreases as g increases for k_3 = 0.8 and k_3 = 2.0, with no resonance occurring. However, for k_3 = 5.0 and k_3 = 10.0, a single resonance is observed, as depicted in Fig. 4(b). Numerical simulations indicate that resonance does not appear for $k_3 < 5.0$, whereas resonance occurs for $k_3 > 5.0$.

Moreover, the possibility of inducing resonance through variations in rate constants k_1 and k_2, in cooperation with the concentration of CO molecules (x), is confirmed by the results presented in Fig. 5. Fig. 5(a) illustrates the dependence of rate constant k1 for three values of ω (= 1, 2, 3), with $\Omega = 30\omega, g = 10$, and f = 0.1. We observe a resonant behavior in which the concentration of CO molecules increases with increasing k_1, reaching a maximum and then decreasing with further increase of k_1. Similar behaviors are observed for ω = 2.0 and 3.0. The variation of rate constant k_2 is shown in Fig. 5(b) for three values of ω (= 1, 2, 3), with $\Omega = 30\omega, g$ = 10, and f = 0.1. Resonant behaviors occur for ω = 1.0 and ω = 2.0, while no resonant behavior is observed at ω = 3.0

We proceed by examining the changes in dynamical behaviors in CO-oxidation over plat inum surfaces (Eq. 6) for three values of k_3, while setting g = 10, Ω = 20ω, and ω = 2.0. Here, we designate f as the bifurcation parameter while keeping g fixed, and the outcomes are depicted in Fig. 6. In Fig. 6(a) and Fig. 6(b), various types of bifurcation phenomena are clearly discernible, encompassing period-doubling, periodic windows, chaos, intermittency, and sudden increases and destructions of chaotic attractors.

The enlargement of Fig. 6(b) is illustrated in Fig. 6(c). Our analysis of Fig. 6 indicates that the variation in k_3 can eradicate chaotic oscillations, periodic windows, and intermittent oscillations when k_3 > 1, while maintaining these phenomena when k_3 < 1.

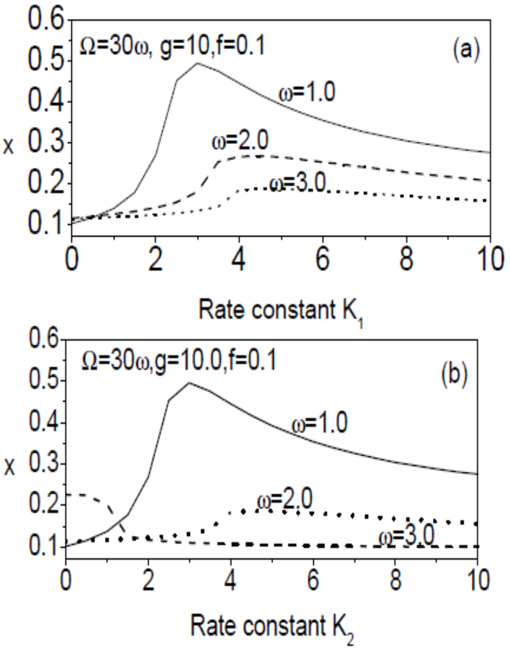

Fig. 5. (a) Variation of the rate constant k_1 with k_2 = 1.5. (b) Variation of the rate constant $k_2$with k_1 = 2.5 with the concentration of *CO* molecules for three values of ω (= 1, 2, 3) respectively. The other parameters are fixed at Ω = 30ω, g = 10, k_3 = 10.0, and f = 0.1

Periodic oscillations emerge solely when k_3 > 1 (Fig. 6d). Subsequently, we investigate the bifurcation phenomena by selecting the parameter g as the bifurcation parameter while keeping f constant. The corresponding numerical results are depicted in Fig. 7 for four different values of ω, with Ω = 20ω and f = 0.1. From this figure, it is evident that no chaotic oscillations occur when we modulate the high-frequency force with the low-frequency force.

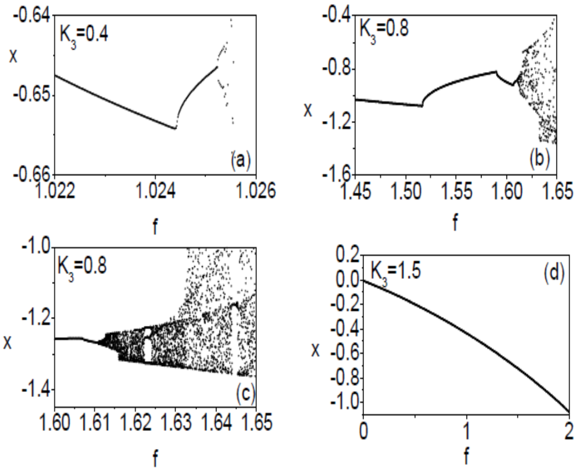

Fig. 6. Bifurcation diagrams of *CO*–oxidation on a platinum catalyst surface model (Eq. 6) for three values of k_3 (= 0.4, 0.8, 1.5) respectively with Ω = 20ω, ω = 2.0, and g = 10.0. Magnification of Fig. 6(b) is shown in Fig. 6(c). Periodic, chaotic, periodic windows, and intermittent oscillations are clearly visible. The values of the other rate constants and the initial conditions are fixed as given in Fig. 1

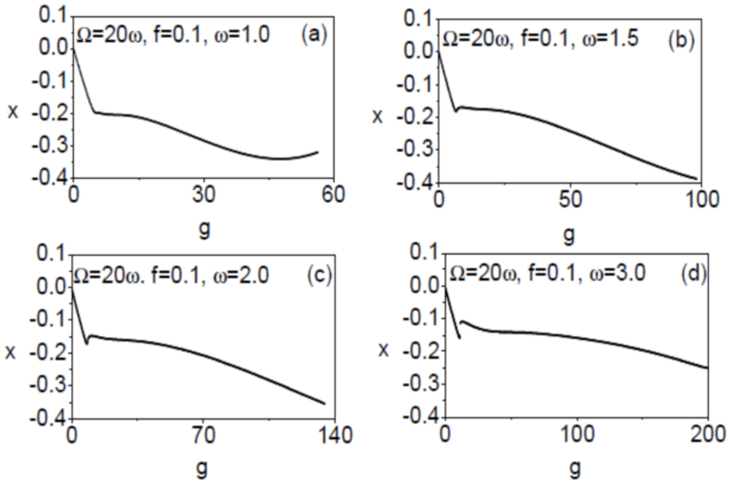

Fig. 7. Bifurcation diagrams of CO–oxidation on a platinum catalyst surface model (Eq. 6) for ω = 1.0, 1.5, 2.0, 3.0 respectively. Periodic oscillations are clearly visible. The values of the rate constants and the initial conditions are fixed as given in Fig. 1

Further, we investigate the influence of the frequencies of the low-frequency force ω and the high-frequency force Ω, as presented in Figs. 8 and 9. First, we examine the occurrence of VR for four different values of the frequency ω of the low-frequency signal. Figure 8 illustrates the variation in the numerically computed response amplitude Q against the control parameter (g), the amplitude of the high-frequency signal, for four fixed values of ω: ω = 1.0, 1.5, 2.0, and 3.0, respectively. The other parameters are set to f = 0.1 and Ω = 20ω. From Fig. 8, we observe single resonance for all the values of ω. The maximum response amplitude Q_{max} decreases as ω increases.

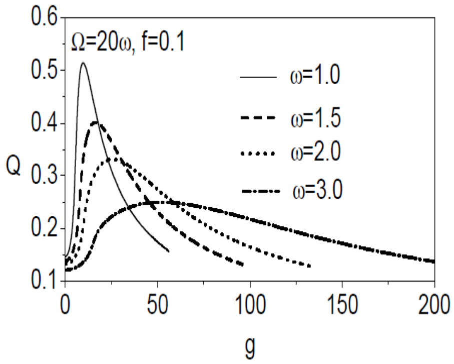

Fig. 8. Response amplitude Q versus g of the kinetic model (Eq. 6) for four values of ω (=1.0, 1.5, 2.0, 3.0) respectively with Ω = 20ω and f = 0.1. The values of the rate constants of the reaction model (Eq. 6) are fixed as follows: k_1 = 2.5, k_{-1} = 1.0, k_3 = 10.0, k_{-2} = 0.1, k_2 = 1.5, k_4 = 2.5, k_{-4} = 1.0, and λ = 0.4. In the numerical calculations, the initial state variables are fixed as x = 0.1, y = 0.8, and s = 0.2.

Additionally, resonance intervals increase and the position of the peaks shifts away from the origin. For example, for ω = 1.0, VR occurs at g = 10.61 with Qmax = 0.5167, at g = 15.22 with Q_{max} = 0.3976 for ω = 1.5, at g = 22.76 with Q_{max} = 0.3239 for ω = 2.0, and at g = 29.67 with Q_{max} = 0.2350 for ω = 3.0. We also observe that chemical oscillations become unbounded when g > 54.90 for ω = 1.0, g > 98.52 for ω = 1.5, and g = 129.67 for ω = 2.0, respectively.

Next, we examine the effect of the frequency (Ω) of the high-frequency signal on VR. The results are presented in Fig. 9, where Q versus g is plotted for three values of Ω with ω = 3.0 and f = 0.1. For all values of Ω, single resonance occurs at different g values with approximately the same Qmax values. As Ω increases, the positions of the peaks shift away from the origin. For Ω = 15ω, motion becomes unbounded when g > 146.96. From Fig. 9, it is evident that at resonance values, the reaction rate increases by facilitating the transfer of CO molecules from the adsorbed state to the gas phase.

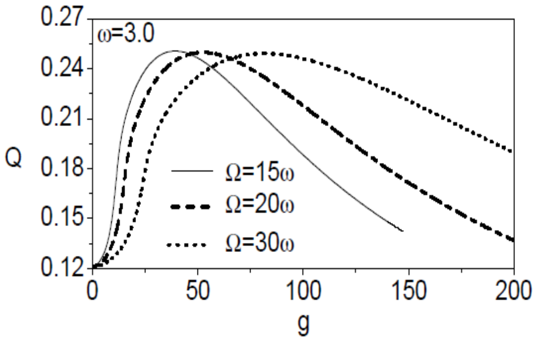

Fig. 9. Response amplitude Q versus g of the kinetic model (Eq. 6) for three values of Ω (= 15ω, 20ω, 30ω) respectively with ω = 3.0 and f = 0.1. The values of the rate constants and the initial conditions are fixed as given in Fig. 1

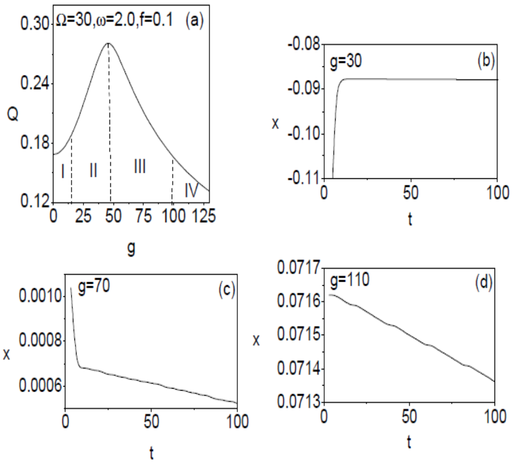

Fig. 10. Response amplitude Q versus g of the kinetic model (Eq. 6) for $\Omega = 30\omega$, $\omega = 2.0$, and $f = 0.1$. (b-d) Trajectory plots corresponding to the regions II, III, and IV in Fig. 10(a). The values of the rate constants and the initial conditions are fixed as given in Fig. 1

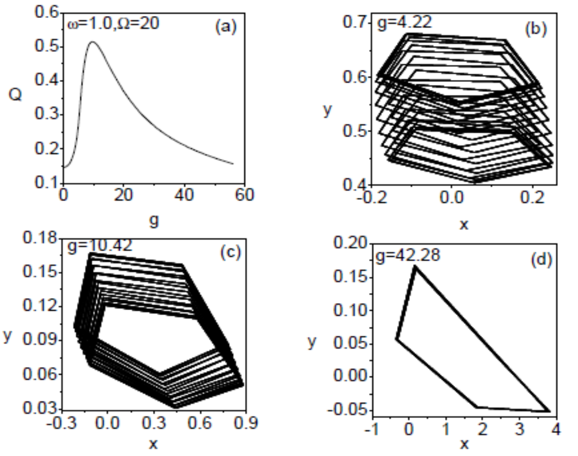

Fig. 11. (a) Response amplitude Q versus g of the kinetic model (Eq. 6) for $\Omega = 20\omega$, $\omega = 1.0$, and $f = 0.1$. (b-d) Phase portraits for three values of g chosen in Fig. 11(a). The chosen values of g are before, at, and far after the resonance. The values of the rate constants and the initial conditions are fixed as given in Fig. 1.

The response curve for $\Omega = 30\omega, \omega = 2$, and $f = 0.1$ is shown in Fig. 10(a). In Fig. 10(a), the resonance region is divided into four intervals. Within these intervals, we study the oscillatory response of the CO-oxidation process over the platinum surface through trajectory plots. The period of the oscillation in the range of g is $T \approx (2\pi/\omega)$. For $g = 30$ (region II), the concentration of CO molecules steadily increases until $t < 10.88$, and after $t > 10.88$, the concentration of CO molecules reaches a steady state, as depicted in Fig. 10(b). For $g = 70$ (region III), the concentration of CO molecules decreases from the maximum and reaches a minimum (Fig. 10(c)), and for $g = 100$ (region IV), the concentration of CO molecules exponentially decreases, as clearly seen in Fig. 10(d). Similarly, the oscillatory behavior of the CO-oxidation over the platinum surface is examined using phase portrait plots in Fig. 11. In Fig. 11(a), we have plotted the response curve for $\omega = 1.0$, $\Omega = 20\omega$, and $f = 0.1$. As the concentration of CO molecules (x) and O_2 molecules (y) increases with increasing g, as depicted in Figs. 11(b), 11(c), and 11(d).

Conclusion

In conclusion, the catalytic oxidation of carbon monoxide (CO) on platinum group metal surfaces stands as one of the most extensively investigated surface-catalyzed reactions, owing to its practical significance in environmental pollution control. Through numerical analysis of a typical surface catalytic reaction model, we observed vibrational resonance behavior when the reaction model is periodically modulated by low-frequency and high-frequency signals. The high-frequency signals play a constructive role in enhancing the low-frequency signal. For specific rate constant values, we identified the occurrence of vibrational resonance for the perturbation parameters f, g, ω, and Ω. At resonant values, the reaction rate increases due to the facilitation of the transition of CO molecules from the adsorbed state to the gas phase.

Furthermore, controlling the vibrational resonance process holds potential for developing more efficient and selective catalysts for various industrial applications. Importantly, due to external periodic perturbation, no hysteresis effects occur in the catalytic CO-oxidation model. The numerical results are elucidated through response amplitude curves, bifurcation diagrams, phase portraits, and trajectory plots, providing valuable insights into the dynamics of CO oxidation over platinum surfaces.

References

[1] Strogatz, S. (2014). *Nonlinear Dynamics and Chaos: With Applications to Physics, Biology, Chemistry, and Engineering*, Ingram Publisher Services US, New York, NY, USA, 2nd edition.

[2] Binous, H., Bellagi, A. (2005). Introducing nonlinear dynamics to chemical and bio- chemical engineering graduate students using Mathematica, *Computer Applications in Engineering Education*, *27*(1), 1–19.

[3] Guruparan, S., Ravindran Durai Nayagam, B., Ravichandran, V., Chinnathambi, V., Rajasekar, S. (2015). Hysteresis, vibrational resonance and chaos

in brusselator chemi- cal system under the excitation of amplitude modulated force, *Chemical Science Reviewand Letters*, *4*(15), 870–879.

[4] Langmuir, I. (1922). The mechanism of the catalytic action of platinum in the reactions $2CO+O_2 = 2CO_2$ and $2H_2+O_2 = 2H_2O$, *Transactions of the Faraday Society*,17.

[5] Epstein, I.R., Pojman, J.A. (1998). *An Introduction to Nonlinear Chemical Dynamics*, Oxford University Press, Oxford, UK,

[6] Showalter, K., Epstein, I.R. (2015). From chemical systems to systems chemistry: pat- terns in space and time, *Chaos: An Interdisciplinary Journal of Nonlinear Science*, *25*(9), 97613-97621.

[7] Rotermund, H.H. (1997). Imaging pattern formation in surface reactions from ultrahigh vacuum up to atmospheric pressures, *Surf. Sci.*, 386, 10.

[8] Imbihl, R., Ertl, G. (1995). Oscillatory kinetics in heterogeneous catalysis, *Chem. Rev.*, 95, 697.

[9] Gong, Y., Hou, Z., Xin, H. (2005). Internal noise stochastic resonance in CO oxidation on nm-sized palladium particles, *Sc. China Ser. B-Chem.*, 48, 395–401. https://doi.org/10.1360/042004-86

[10] Frster, A., Merget, M., Schneider, F.W. (1996). Stochastic Resonance in Chem- istry. The Peroxidase-Oxidase Reaction, *J. Phys. Chem.*, *100*(11), 4442–4447. https://doi.org/10.1021/jp952244p

[11] Yang, L., Hou, Z., Zhou, B., Xin, H. (1996). Stochastic resonance in catalytic reduction of *NO* with *CO* on Pt.100, *J. Chem. Phys.*, *109*(15), 6456–6459.

[12] Yang, L., Hou, Z., Xin, H. (1998). Stochastic resonance in surface catalytic oxidation of carbon monoxide, *J. Chem. Phys.*, 109(5), 2002–2005.

[13] Ma, J., Hou, Z., Gao, Q. (2012). Two-parameter coherent resonance behavior in catalytic oxidation of CO on platinum surface, *Physics Letters A*, *376*(4), 426–431. 10.1016/j.physleta.2011.11.029

[14] Landa, P.S., McClintock, P.V.E. (2000). Vibrational resonance. *J. Phys. A: Math. Gen. 33*(45), L433–438.

[15] Gittermann, M., (2001). Bistable oscillator driven by two periodic fields. *J. Phys. A: Math. Gen., 34*(24), L355–357.

[16] Blekhman, I.I., Landa, P.S. (2004). Conjugate resonances and bifurcations in nonlinear systems under biharmonical excitation. *Int. J. Nonlin. Mech. 39*(3), 421–426.

[17] Agaoglu, S.N., Calim, A., Hoevel, P., Ozer, M. Uzuntarla, M., (2019). Vibrational resonance in a scale-free network with different coupling schemes, *Neurocomputing*, 325, 59–66. doi:10.1016/j.neucom.2018.09.070.

[18] Uzuntarla, M., Yilmaz, E., Wagemakers, A., Ozer, M. (2015). Vibrational resonance ina heterogeneous scale free network of neurons, *Commun. Nonlinear Sci. Numer. Simul.*22, 367–374. doi:10.1016/j.cnsns.2014.08.040.

[19] Hu, D.L., Yang, J.H., Liu, X.B. (2014). Vibrational resonance in the FitzHugh- Nagumo system with time-varying delay feedback, *Comput. Biol. Med.*, 45, 80–86. doi:10.1016/j.compbiomed. 2013.11.022.

[20] Roy-Layinde, T.O., Laoye, J.A., Popoola, O.O., Vincent, U.E., (2016). Analysis of vibrational resonance in bi-harmonically driven plasma, *Chaos 26*(9), 093117. https://doi.org/10.1063/1.4962403.

[21] Enjieu Kadji, H.G., Nana Nbendjo, B.R., Chabi Orou, J.B., Talla, P.K. (2008). Nonlinear dynamics of plasma oscillations modeled by an anharmonic oscillator, *Phys. Plas- mas*, 15, 032308. https://doi.org/10.1063/1.2841032

[22] Bhuvaneshwari, B., Amutha, B., Chinnathambi, V., Rajasekar, S. (2021). Enhanced vibrational resonance by an amplitude modulated signal in a nonlinear dissipative two-fluid plasma model, *Contrib. Plasma Phys.*, e202100099, 1–10 https://doi.org/10.1002/ctpp.202100099.

[23] Chizhevsky, V.N. (2021). Amplification of optical signals in a bistable vertical-cavity surface-emitting laser by vibrational resonance, *Philos. Trans. R. Soc. A*, 379, 20200241. doi: 10.1098/rsta.2020.0241

[24] Chizhevsky, V.N., Smeu, E., Giacomelli, G. (2003). Experimental evidence of vibrational resonance in an optical system, *Physical Review Letters*, *91*(22), 220602/1- 220602/4CODEN: PRLTAO.

[25] Chizhevsky, V.N., Giacomelli, G. (2005). Improvement of signal-to-noise ratio in a bistable optical system: Comparison between vibrational and stochastic resonance, *Phys. Rev. A: At., Mol., Opt. Phys.*, *71*, 011801. doi: 10.1103/PhysRevA.71.011801

[26] Kurzin, V.B. (1972). Acoustic resonance associated with vibrations of an array of plates in a subsonic flow, *Fluid Dyn.*, 7, 822–826. https://doi.org/10.1007/BF01205762

[27] Omoteso, K.A., Roy-Layinde, T.O., Laoye, J.A., Vincent, U.E., McClintock, P.V.E. (2021). Acoustic vibrational resonance in a Rayleigh-Plesset bubble oscillator, *Ultrasonics Sonochemistry*, 70, 105346, https://doi.org/10.1016/j.ultsonch.2020.105346

[28] Kolebaje, O.T., Vincent, U.E., Benyeogor, B.E., McClintock, P.V.E., Kolebaje, O.T. (2023). U. Effect of a modulated acoustic field on the dynamics of a vibrating charged bubble, *Ultrasonics*, 135., 107110. doi:10.1016/j.ultras.2023.107110.

[29] Guruparan, S., Ravindran Durai Naayagam, B., Jeyakumari, S., Chinnathambi, V. (2015). Effect of different shape of periodic forces on chaotic oscillation in Brusselator Chemical system, *Int. Journal of Computational and Theoretical Chemistry*, *3*(3), 19–27.

[30] Monwanou, A.V., Koukpem'edji, A.A., Ainamon, C., Nwagoum Tuwa, P.R., Miwadi- nou, C.H., Chabi Orou, J.B. (2020). Nonlinear Dynamics in a Chemical Reaction under an Amplitude-Modulated Excitation: Hysteresis, Vibrational Resonance, Multi- stability, and Chaos, *Hindawi Complexity*, *2020*, 8823458, https://doi.org/10.1155/2020/8823458.

[31] Shabunin, A., Astakhov, V., Demidov, V. (2003). Modeling chemical reactions by forced limit-cycle oscillator: synchronization phenomena and transition to chaos, *Chaos, Solitons* & *Fractals*, *15*(2), 395–405.

[32] Lashina, E.A., Slavinskaya, E., Kibis, L., Stadnichenko, A., Stonkus, O., Zhuravlev, D., Zadesenets, A., Korenev, S., Podyacheva, O., Boronin A. (2023). CO Oxidation Reaction by Platinum Clusters on the Surface of Multiwalled Carbon Nanotubes: Experi- mental and Theoretical Study of Kinetics in a Wide Range of O_2/CO Ratios, *Catalysts*, *13*(3), 568. https://doi.org/10.3390/catal13030568

[33] Lashina, E.A., Chumakova, N.A., Chumakov, G.A., Boronin. A.I. (2009). Chaotic dynamics in the ‚three-variable kinetic model of CO oxidation on platinum group metals, Chemical *Engineering Journal*, *154*(1-3), 82–87.

https://doi.org/10.1016/j.cej.2009.02.017.

[34] Kapicka, J., Marek, M. (1989). Transition to Chaos in the Oscillating Co oxidation on P t/Al203, *Surface Science*, 222, L885–L889.

[35] Thangapandi, C., Rajendran L. (2013). Analytical expression of concentrations of adsorbed CO molecules, O atoms and oxide oxygen, *Natural Science, 5*(3), 326–332. doi:10.4236/ns.2013.53045.

[36] Elokhin, V.I., Matveev A.V., Gorodetskii V.V. (2009). Self-Oscillations and Chemical Waves in CO Oxidation on Pt and Pd: Kinetic Monte Carlo Models, *Kinetics and Catalysis, 50*(1), 40–47.

[37] Xiang-Hong, Li., Qin-Sheng, Bi. (2013). Forced bursting and transition mechanism in CO oxidation with three time scales, *Chin. Phys. B, 22*(4), 040504.

[38] Latkin E.I., Elokhin V.I., Gorodetskii V.V. (2001). Monte Carlo model of oscillatory CO oxidation having regard to the change of catalytic properties due to the adsorbate- induced Pt(1 0 0) structural transformation, *Journal of Molecular Catalysis A: Chem- ical, 166*(1), 23–30. https://doi.org/10.1016/S1381-1169(00)00468-4.

[39] Kurkina, E.S., Semendyaeva, N.L. (2005). Oscillatory dynamics of CO oxidation on platinum-group metal catalysts, *Kinetics and Catalysis, 46*, 453–463. doi:10.1007/s10975-005-0098-4

[40] Engel, T., Ertl, G. (1979). Elementary steps in the catalytic oxidation of carbon monoxide on platinum metals, *Adv. Catal., 28*, 1–78.